

Research Article

A Simple Approach to Distinguish Classic and Formaldehyde-Free Tannin Based Rigid Foams by ATR FT-IR

Gianluca Tondi,¹ Martin Link,¹ Chuan Wei Oo,² and Alexander Petutschnigg¹

¹Forest Products Technology & Timber Construction Department, Salzburg University of Applied Sciences,
136a Marktstraße, 5431 Kuchl, Austria

²School of Chemical Sciences, Universiti Sains Malaysia (USM), 11800 Penang, Malaysia

Correspondence should be addressed to Gianluca Tondi; gianluca.tondi@fh-salzburg.ac.at

Received 9 October 2014; Accepted 9 February 2015

Academic Editor: Eugen Culea

Copyright © 2015 Gianluca Tondi et al. This is an open access article distributed under the Creative Commons Attribution License, which permits unrestricted use, distribution, and reproduction in any medium, provided the original work is properly cited.

Tannin based rigid foams (TBRFs) have been produced with formaldehyde since 1994. Only recently several methods have been developed in order to produce these foams without using formaldehyde. TBRFs with and without formaldehyde are visually indistinguishable; therefore a method for determining the differences between these foams had to be found. The attenuated total reflectance infrared spectroscopy (ATR FT-IR) investigation of the TBRFs presented in this paper allowed discrimination between the formaldehyde-containing (classic) and formaldehyde-free TBRFs. The spectra of the formaldehyde-free TBRFs, indeed, present decreased band intensity related to the C–O stretching vibration of (i) the methylol groups and (ii) the furanic rings. This evidence served to prove the chemical difference between the two TBRFs and explained the slightly higher mechanical properties measured for the classic TBRFs.

1. Introduction

Tannin based rigid foams (TBRFs) are innovative materials obtained by exploiting the capacity of tannin for undergoing polyaddition reactions and that of furfuryl alcohol to polymerize under acid catalysis [1–3]. These materials have been investigated for many years, but only recently have they been systematically studied and many of their properties have been evaluated [4–7].

The first generation of TBRFs has shown good insulation properties and outstanding resistance against fire but they were produced with around 5% of formaldehyde, required to keep the network stable at room temperature. This drawback has hindered the development of the foams for industrialization because formaldehyde was the most debated chemical in wood science until it was classified as a carcinogenic molecule by the IARC in 2006 [8].

Therefore, several efforts were made in order to produce 100% natural foams [9, 10] without formaldehyde. It was discovered that, by applying an external energy source, the formaldehyde-free tannin-furanic polymer could cross-link to similar extent and the new material obtained had similar

properties to the first generation foams [11–13]. In addition, the new TBRFs had a fully natural profile and they were proven to be suitable for the production of lightweight panels; their mechanical performances are slightly weaker than the formaldehyde-containing TBRFs.

Numerous investigations have been carried out to clarify the chemistry of the tannin-furanic polymers, but only partial information could be achieved [14–17]. On one hand, the flavonoid tannin extracts are constituted of aromatic oligomers variously substituted with hydroxyl groups [18, 19] and on the other hand the furanic polymers derived from acid polymerization of furfuryl alcohol present strongly interconnected networks in which the π -electrons can be involved in unpredictable Diels-Alder reactions [20, 21]. The NMR and the MALDI-TOF studies as well as previous investigations were not able to unscramble the polymerization process completely.

In the present paper, the attenuated total reflectance (ATR) infrared spectroscopy was used to investigate the TBRFs and to discriminate the innovative formaldehyde-free TBRFs from the classic TBRFs produced with formaldehyde.

TABLE 1: Composition by weight of classic and formaldehyde-free tannin based rigid foams.

Chemicals	Classic TBRFs (%) Room temperature	Formaldehyde-free TBRFs (%) Hot press at 120°C
Mimosa tannin	47.7	52.6
Furfuryl alcohol	16.7	13.1
Formaldehyde	4.3	—
Blowing agent	4.8	3.5
Acid catalyst	12.4	5.8
Water	14.1	25.0

2. Experimental

2.1. Materials. The polymers investigated in the present study were produced with the following chemicals: mimosa tannin (*Acacia mearnsii* formerly *mollissima*) extract and furfuryl alcohol, which were kindly provided by Silva Chimica (Italy) and International Furan Chemicals (Holland), respectively. The other chemicals, namely, formaldehyde solution (ca 37%), diethyl ether (blowing agent), and sulphuric acid (acid catalyst), were supplied by Lactan.

2.2. Polymer Preparation. The mimosa tannin-formaldehyde polymer (TF) was produced by mixing a tannin solution in water (50%) with 10% formaldehyde (w/w) in a plastic test tube. Some drops of sulphuric acid 30% were added to adjust the pH to 2.0. After vigorous mixing, the test tube was sealed with a screw cap and the solution was kept in the oven at 103°C for 24 hours. The resulting polymer was crushed in powder and further dried for 2 hours in a ventilated oven at 60°C.

The polyfurfuryl alcohol (PFA) was prepared by adding a few drops of sulphuric acid 30% to 2 g of furfuryl alcohol. The exothermic polymerization reaction took place in a few seconds producing a black polymer. The polymer was then ground and dried for 2 hours at 60°C.

The classic tannin based rigid foams were produced with formaldehyde at room temperature while the formaldehyde-free tannin based rigid foams were produced at 120°C, heating the sample with the hot plates of a press. The two foams were produced according to the protocols already published elsewhere [2, 10]. Sulphuric acid 30% was used instead of p-toluenesulfonic acid (65%) for the synthesis of the TBRFs. The chemical composition of the two formulations is reported in Table 1.

The TBRFs were cut into small specimens of around $2 \times 2 \times 2$ cm³ dimension keeping only the core material and successively conditioned at 20°C and 65% m.c. for more than one month. Finally, the foams were crushed in a mortar and kept for 5 minutes in a ventilated oven at 60°C, before ATR FT-IR investigation.

2.3. ATR FT-IR Spectroscopy. The finely ground powders were analysed with a Frontier FT-IR spectrometer from Perkin-Elmer equipped with a Miracle diamond ATR unit. The investigations were performed in absorbance with 32 scans in the

spectral area between 4000 and 600 cm⁻¹ with a resolution of 4 cm⁻¹. The measurements were repeated 5 times for each batch and the spectra obtained were then elaborated with the software “Unscrambler” by Camo. Baseline correction and vector normalization of the signals were applied before averaging the 5 spectra for each sample.

3. Results and Discussion

The classic tannin based rigid foams (classic TBRFs) are copolymers constituted by flavonoid tannin, formaldehyde, and furfuryl alcohol units as monomers. The way in which these monomers are interconnected in the TBRFs is still nebulous. Considering that tannin can copolymerize with formaldehyde and that furfuryl alcohol can homopolymerize to polyfurfuryl alcohol (PFA), the TBRFs can be approached as a combined copolymer between these two basic polymers. Figure 1 shows the ATR FT-IR spectra of tannin-formaldehyde polymer (TF), polyfurfuryl alcohol (PFA), and classic tannin based rigid foam (classic TBRF). The specific bands attributed to these spectra are reported in Table 2.

The broad band in the region of 3700 to 3000 cm⁻¹ showed the stretching vibration of the O–H groups in the different molecules. Comparing the intensity of this band for the three polymers, PFA contained the lowest amount of O–H group since most hydroxyl groups from the furfuryl alcohol monomers were removed via dehydration during the polycondensation reactions to form PFA. The more structured spectrum of the PFA was observed also for other furanic molecules as in Table 2. Burket et al. reported the stretching of C–H in complex furanic polymers absorbed at these wavenumbers [22]. Bands at around 2900 cm⁻¹ indicated the presence of saturated C–H stretching from the methylene (–CH₂–), dimethylene ether (–CH₂–O–CH₂–), and methylol (–CH₂OH) groups in the TF, PFA and classic TBRF. The region between 2500 and 1800 cm⁻¹ does not present significant absorptions except for CO₂ and therefore it can be negligible.

At around 1700 cm⁻¹ the C=O bond stretching occurs. All the polymers studied present a large band at this wavenumber. The tannin extracts show this peak exclusively after formaldehyde activation [23], while the furanic polymer presents carbonyl groups after furan ring opening for incomplete scission of the ether linkage. The possible structure of PFA with the opened furan ring (Figure 2) has been suggested by Conley and Metil [24]. The presence of this signal in the classic TBRF also meant that carbonyl groups were still available after the reaction was completed.

The absorption at around 1610 cm⁻¹ is very intense for the tannin-containing polymers while being less significant for the polyfurfuryl alcohol. This peak is typically attributed to C=C stretching in benzene ring. The formation of the aromatic benzene rings in PFA could occur from the Diels-Alder reactions between the furan rings (dienes) in an oligomeric chain and conjugated dihydrofuranic sequences (dienophiles) in another oligomer chain [20]. The Diels-Alder adducts could further undergo aromatization converting the oxygen-bridged bicyclic moiety into the benzene ring (Figure 3). The newly formed benzene rings linked the two

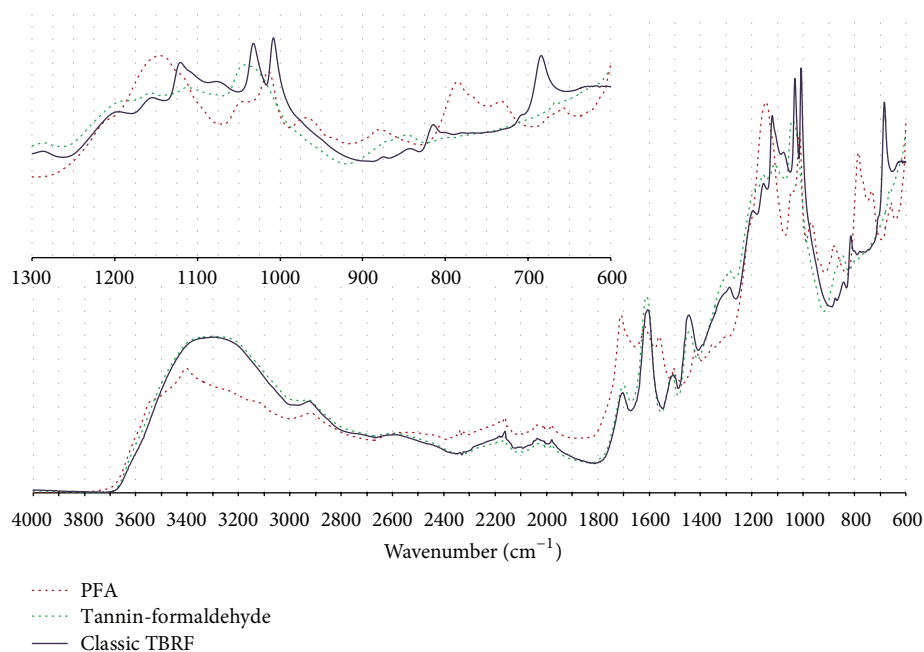


FIGURE 1: ATR FT-IR spectra of polyfurfuryl alcohol (red dot) tannin-formaldehyde polymer (green dots) and classic tannin based rigid foam (dark blue).

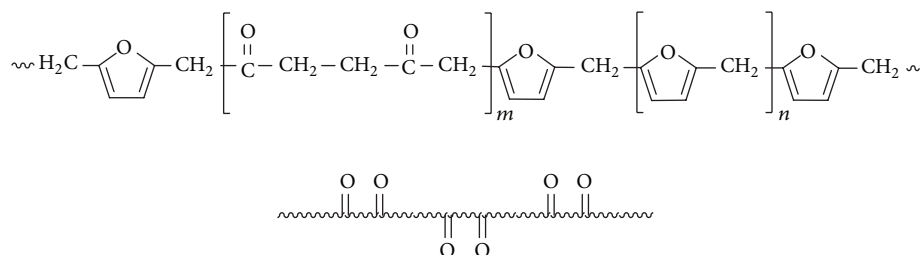


FIGURE 2: Structure of polyfurfuryl alcohol (PFA) with opened furan ring [23].

PFA chains together and enhanced the conjugation of the polymeric system.

The spectral region between 1560 and 1300 cm^{-1} presents principally in-plane C–H bending of aromatic molecules. The heteroaromatic compounds absorb preferentially in the region 1560–1500 cm^{-1} while the phenolic compounds present major vibrations at around 1450 cm^{-1} .

The region between 1300 and 950 cm^{-1} (expanded in Figure 1) is strongly dominated by C–O stretching vibrations even if a few O–H bending and aromatic C–H bending vibrations occurred as well. In this region of the spectrum, the classic TBRF presents a slightly different profile from the ones of the two templates polymers. A major disaccord occurred at 1120 cm^{-1} where the –C–O–C– stretching signal takes place. This band shows higher intensity due to the increasing amount of ether bridges in the TBRF. This assumption could be confirmed noticing the increase of the bands at around 1035 and 1010 cm^{-1} . These bands could be attributed to C–O vibrations of (i) –C–O–C– ether bridges in complex oxygen containing cyclic molecules and/or (ii) =C–O–C= breathing in furanic moieties. The first confirmed

the presence of dimethylene-ether bridges obtained by the condensation of two methylol groups, while the second suggested a lower degree of furan ring opening when the PFA polymerized in presence of tannin-formaldehyde at room temperature. It is worth noting that the TF polymerized also via methylol condensation, but due to the drastic polymerization conditions (103°C for 24 hours) the higher majority of the dimethylene-ether bridges evolved to methylene bridges by releasing formaldehyde.

In the fingerprint region from 950 to 600 cm^{-1} the assignments are very complicated but C–H bending of aromatic (principally out of plane) occurs with high frequency. This region can give immediate information about the degree of compactness of the polymers. The more the polymer is compactly networked, the less the absorption for out-of-plane vibration will be due to the high steric hindrance. The classic TBRF FT-IR spectrum presents intermediate compactness between TF (highly interconnected) and PFA (less interconnected). Distinct signals between TBRF and the two basic polymers (PFA and TF) could be observed especially at the wavenumbers 780 and 680 cm^{-1} . The strong signal at

TABLE 2: FT-IR absorption bands of the tannin and furanic polymers.

Peaks (cm^{-1})	Tannin-formaldehyde polymer (TF)	Polyfurfuryl alcohol (PFA)	Classic TBRF	Formaldehyde-free TBRF	Template compounds*	Assignments
3545–3405		L			Furfural, furfuryl alcohol, pyrogallol.	O–H stretch.
3280	L		L	L	Phenol, resorcinol, benzyl alcohol, furfuryl alcohol, pyrogallol, catechin, flavanol.	O–H stretch.
3100		S			phenol, benzaldehyde, furfural, furfuryl alcohol, benzofuran, flavanol, diphenylmethane.	C–H stretch. Aromatics, also PFA [22]
2920	M	M	M	M	Methanol, diethyl ether, benzyl alcohol, furfuryl alcohol, catechin, diphenylmethane.	C–H stretch. Aliphatics [22].
1710	L	L	L	L	Benzaldehyde, furan, furfuryl alcohol, benzofuran.	C=O stretch (furan ring opening), formaldehyde activated tannin.
1610	L	M	L	L	Phenol, resorcinol, benzyl alcohol, catechin, benzofuran, flavanol, diphenylmethane.	C=C stretch. Aromatics (6C) [22, 25] also flavonoids [25].
1560		M			Furfuryl alcohol, flavanol, benzofuran, diphenylmethane.	C=C–H stretch. symm. aromatic (in-plane) [26] also furanics [22, 27].
1505		S	M	M	Phenol, guaiacol, benzofuran, furfuryl alcohol.	C=C–H stretch. asym. aromatic (in-plane) [27] also furanics [22, 27].
1450	L		L	L	Resorcinol, benzyl alcohol, benzaldehyde, furfural, pyrogallol, catechin, flavanol, diphenylmethane.	C–H bend. asym. aromatic [22, 28] also flavonoids [29], C–O stretch. Aromatic (6C) [17].
1420		S			Furfuryl alcohol, flavanol, diphenylmethane.	C–H bend. In-plane O-containing aromatics; C=C stretch ring B [25]
1360		S			Benzyl alcohol, furfural, furfuryl alcohol, benzofuran, pyrogallol, catechin, flavanol.	C–H bend. symm. in-plane aromatic conjugated sequences of polymer backbones.
1290	M	S	M	M	Phenol, resorcinol, benzaldehy., pyrogallol, catechin, flavanol.	C–O stretch. Aromatics (6C) [25] (also ring B of flavonoids) [29].
1210	M		S	S	Benzyl alcohol, guaiacol, flavanol.	O–H bend. in-plane deformation.
1160	S	L	M	M	Phenol, resorcinol, guaiacol, furan, furfural, furfuryl alcohol, benzofuran, pyrogallol.	C–O stretch. Aromatics [25, 27] also ring A of flavonoids and also furanics; H–C–C bend. Ring B [25].
1120			M	S	Methanol, diethyl ether, guaiacol, catechin, flavanol.	C–O stretch. Aliphatic, methylene-ether bridges. [27]
1080	L		S		Phenol, resorcinol, benzaldehyde, furfural, furfuryl alcohol, catechin, flavanol.	C–H bend. also ring B of flavonoids [28, 29]; =C–O–C= stretch [17, 27].
1035		S	L	L	Benzofuran.	=C–O–C= stretch [27, 28]. Breathing oxoaromatic compounds.
1010	S	M	L		Furfural, furfuryl alcohol, benzofuran.	=C–O–C= stretch [17]. Breathing oxoaromatic compounds, methylene-ether bridges and methoxy activation.
970		M			Resorcinol, furan, furfuryl alcohol, catechin.	C–O stretch. Aromatic (6C) also flavonoids [17, 25, 29] and C–H bend. aromatic Out-of-plane asym.
880		M	S	S	Phenol, furfural, furfuryl alcohol, catechin, flavanol.	C–H bend. out-plane asym., also furanics.
840			S	S	Resorcinol, benzyl alcohol, furfural, pyrogallol.	C–H bend aromatic out-plane asym [28].
810			S		Benzyl alcohol, catechin.	C–H bend. aromatic out-plane symm.
780		L			Benzofuran, naphthalene.	C–H bend. aromatic out-of-plane conjugated furanics.
730		S			Resorcinol, benzyl alcohol, difurfuryl ether, furfural, pyrogallol.	C–C–C ring bend. symm., C–H bend. out-of-plane symm. [28]. Also furanics.
680			L		Phenol, resorcinol, benzaldehyde, catechin, flavanol.	C–C–C ring in-plane stretch. C–H bend. out-of-plane symm. (6C) [21].
650		S			Methylfuran, naphthalenediols.	C–C–C ring in-plane stretch. Conjugated aromatics.

* According to the Spectral Database for Organic Compounds SDBS (http://sdb.sdb.aist.go.jp/sdbs/cgi-bin/direct_frame_top.cgi).

L = large; M = medium; S = small.

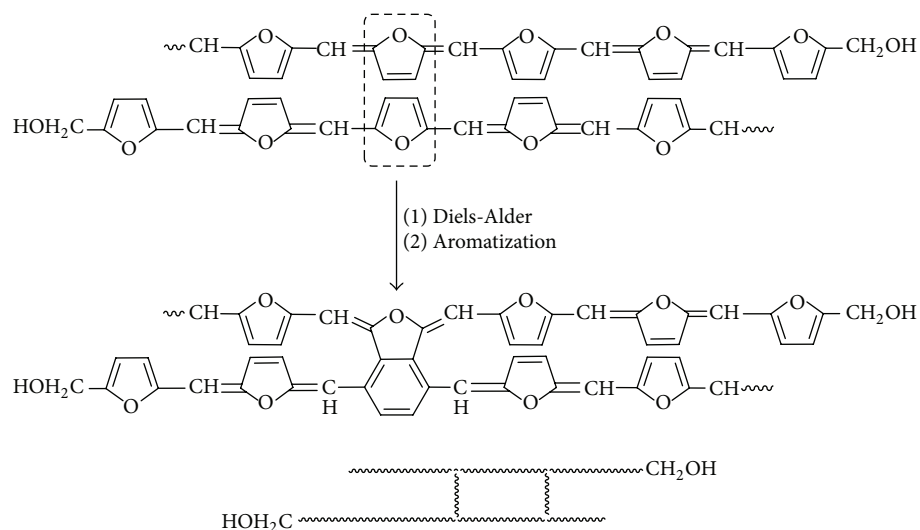


FIGURE 3: Formation of benzene ring via the Diels-Alder and aromatization reactions joining the two polyfurfuryl alcohol chains.

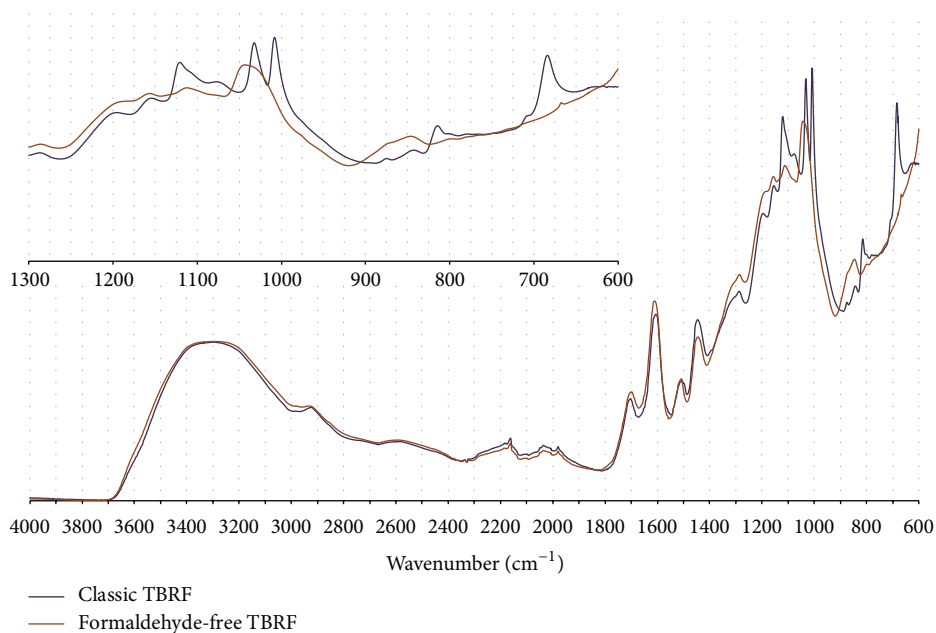


FIGURE 4: ATR FT-IR spectra of classic (blue) and formaldehyde-free (brown) tannin based rigid foam.

780 cm⁻¹ of PFA which can be attributed to the conjugated polyheteroaromatic furan ring decreased due to the limited amount of ring opening. Classic TBRF showed a strong absorption at 680 cm⁻¹ referring to the C–C–C ring in-plane stretching and C–H out-of-plane bending of the benzene rings. Comparing the TF and classic TBRE, some of the tannin-formaldehyde copolymers in classic TBRF were interacted with the terminal methylol groups of PFA (Figure 3) which separated the tannin-formaldehyde copolymers from each other. This orientation reduced the compactness of polymers arrangement in classic TBRF that made the C–C–C stretching and C–H bending occur more easily. The tannin-formaldehyde copolymers in TF, however, had higher compact arrangement that hindered these vibration modes.

PFA also showed small absorption at 680 cm⁻¹ due to the formation of small amount of benzene rings from the Diels-Alder and aromatization reactions between the PFA chains.

In summary, the vibrations of the classic TBRF could be obtained as a mix between the tannin-formaldehyde copolymer and the polyfurfuryl alcohol for all over the middle infrared region. It was possible to consider two extreme scenarios: (i) the two basic polymers were not competitive and developed in a parallel way without copolymerizing each other and (ii) the three monomers mixed intimately but maintained the structure similarly arranged to the two basic copolymers. Due to the fact that only a few “partially new” bands were observed (1120, 1035, and 1010 cm⁻¹), it could be more logical to consider scenario (i) as the one occurring

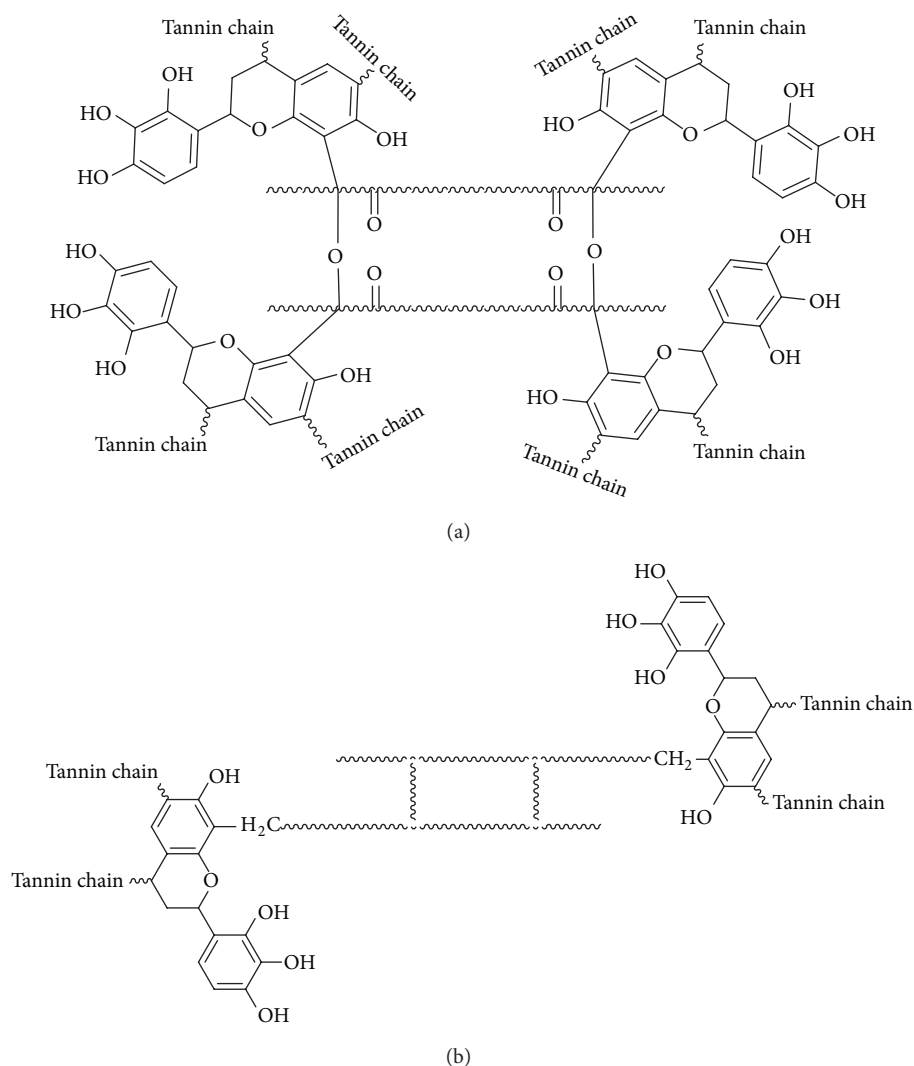


FIGURE 5: Proposed tannin-furanic interactions in formaldehyde-free TBRF (a) and classic TBRF (b).

to the higher extent. But considering the fast kinetics of the formation of furanic polymers, it is sensible to imagine that a certain amount of tannin molecules incorporated into the network of the polyfurfuryl alcohol can create some covalent bonded tannin-furanic adducts preferentially via dimethylene ether ($-\text{CH}_2-\text{O}-\text{CH}_2-$) bridges. The FT-IR investigation of the tannin foams showed that the MALDI-TOF investigations are mostly confirmed: even if a certain amount of units in which furanics and flavonoids are combined, most of the copolymers are constituted of tannin-formaldehyde or polyfurfuryl alcohol fractions. These considerations become more interesting when formaldehyde-free tannin foams are investigated.

Indeed, when the spectra of classic TBRF and formaldehyde-free TBRF are compared (Figure 4), it is possible to notice that from 4000 until 1200 cm^{-1} the spectra overlap almost perfectly. Due to the lack of formaldehyde, the signal at 1700 cm^{-1} could have been significantly decreased for formaldehyde-free TBRF, but no evidence of

this phenomenon occurs, because the carboxyl group was predominantly derived from the incomplete scission of the furfuryl alcohol's units.

Conversely, a certain difference takes place in the wavenumber region between 1200 and 600 cm^{-1} . The main difference can be attributed to lack of the band at 1010 cm^{-1} and the decreasing intensity of the bands at 1120 , 1080 , 810 , and 680 cm^{-1} for formaldehyde-free TBRF. The band at 1010 cm^{-1} could be attributed to the bending of dimethylene-ether bridges formed when the tannin reacted with the formaldehyde. This band was strongly decreased in the formaldehyde-free TBRF spectrum. This first observation combined with the decreasing of the band intensity at 1120 cm^{-1} suggested that dimethylene-ether bridges were strongly diminishing in formaldehyde-free TBRF. The presence of this signal, even if to a small extent, suggested that other ether bridges could occur also from the tannin-furanic interaction as shown in Figure 5(a). Finally further evidence occurring in the formaldehyde-free TBRF is the reduced

intensity of the band at 1080 cm^{-1} which corresponds to the $=\text{C}-\text{O}-\text{C}=$ breathing of the furanic ring and suggested that the furfuryl alcohols, when polymerized at higher temperature (120°C), have a higher tendency to break their ring structure. Much weaker bands at 810 and 680 cm^{-1} suggested less aromatic C–H out-of-plane vibration. This could be due to the more compact tannin-furanic network in formaldehyde-free TBRF which hindered this kind of C–H vibration.

Generally, it can be assumed that formaldehyde-free TBRF and classic TBRF present different polymerization systems. For formaldehyde-free TBRF, the furanic rings were more easily opened to reveal the reactive sites (C=O groups), creating certain amount of flavonoid-furan interconnections which were structurally close to each other so that the aromatic parts of the polymer had higher difficulties in vibrating (Figure 5(a)). As for the classic TBRF, the methylol groups of tannin polymers could be reacted with the free hydroxyl groups at both terminal ends of the benzene linked PFA chains giving greater space among the aromatic parts (Figure 5(b)). This molecular arrangement suggested that the formaldehyde-free TBRF was even more brittle and hence less mechanically performing.

4. Conclusions

Infrared spectroscopy has shown to be a very good method for the investigation of tannin based rigid foams. In particular it was possible to confirm the MALDI-TOF study for the classic TBRF in which the presence of a majority of tannin-formaldehyde and polyfurfuryl alcohol with which only some evidence of simultaneous presence of the three constituents was detected.

The formaldehyde-free TBRF can be discriminated from the classic TBRF by ATR FT-IR spectroscopy. The fingerprint region (between 1200 and 600 cm^{-1}) of their FT-IR spectra offered small but significant differences. The higher temperature at which the formaldehyde-free TBRFs were produced allowed more furanic units to open their rings, increasing the amount of branches from the tannin-furanic interactions. Tannin-furanic interactions in formaldehyde-free TBRF created more compact polymeric system which involves a more rigid structure compared to the classic TBRF. This evidence explains the weaker mechanical properties of formaldehyde-free TBRF.

Conflict of Interests

The authors declare that there is no conflict of interests regarding the publication of this paper.

Acknowledgment

The authors gratefully acknowledge the federal state of Salzburg for its support in the project “Enhancing the Properties of Biogenic Materials for Their Application in Green Building Insulation.”

References

- [1] N. E. Meikleham and A. Pizzi, “Acid- and alkali-catalyzed tannin-based rigid foams,” *Journal of Applied Polymer Science*, vol. 53, no. 11, pp. 1547–1556, 1994.
- [2] G. Tondi and A. Pizzi, “Tannin-based rigid foams: characterization and modification,” *Industrial Crops and Products*, vol. 29, no. 2–3, pp. 356–363, 2009.
- [3] G. Tondi, W. Zhao, A. Pizzi, G. Du, V. Fierro, and A. Celzard, “Tannin-based rigid foams: a survey of chemical and physical properties,” *Bioresource Technology*, vol. 100, no. 21, pp. 5162–5169, 2009.
- [4] G. Tondi, C. W. Oo, A. Pizzi, A. Trosa, and M. F. Thevenon, “Metal adsorption of tannin based rigid foams,” *Industrial Crops and Products*, vol. 29, no. 2–3, pp. 336–340, 2009.
- [5] G. Tondi, A. Pizzi, and R. Olives, “Natural tannin-based rigid foams as insulation for doors and wall panels,” *Maderas: Ciencia y Tecnologia*, vol. 10, no. 3, pp. 219–227, 2008.
- [6] G. Tondi, M. Johansson, S. Leijonmark, and S. Trey, “Tannin based foams modified to be semi-conductive: synthesis and characterization,” *Progress in Organic Coatings*, vol. 78, pp. 488–493, 2015.
- [7] G. Tondi, S. Blacher, A. Leonard et al., “X-ray microtomography studies of tannin-derived organic and carbon foams,” *Microscopy and Microanalysis*, vol. 15, no. 5, pp. 384–394, 2009.
- [8] IARC, “Formaldehyde, 2-Butoxyethanol and 1-tert-Butoxypropan-2-ol,” Group 1, 88, 100F, 2006, <http://monographs.iarc.fr/ENG/Classification/>.
- [9] M. C. Basso, X. Li, V. Fierro, A. Pizzi, S. Giovando, and A. Celzard, “Green, formaldehyde-free, foams for thermal insulation,” *Advanced Materials Letters*, vol. 2, no. 6, pp. 378–382, 2011.
- [10] C. Lacoste, M. C. Basso, A. Pizzi, M.-P. Laborie, D. Garcia, and A. Celzard, “Bioresourced pine tannin/furanic foams with glyoxal and glutaraldehyde,” *Industrial Crops and Products*, vol. 45, pp. 401–405, 2013.
- [11] M. Link, C. Kolbitsch, G. Tondi, M. Ebner, S. Wieland, and A. Petutschnigg, “Tannin-based foams for panels,” *Bioresources*, vol. 6, pp. 4218–4228, 2011.
- [12] C. Kolbitsch, M. Link, A. Petutschnigg, S. Wieland, and G. Tondi, “Microwave produced tannin-furanic foam,” *Journal of Materials Research*, vol. 1, no. 3, pp. 84–91, 2012.
- [13] G. Tondi, M. Link, C. Kolbitsch, and A. Petutschnigg, “Infrared-catalyzed synthesis of tannin-furanic foams,” *BioResources*, vol. 9, no. 1, pp. 984–993, 2014.
- [14] G. Tondi, A. Pizzi, H. Pasch, and A. Celzard, “Structure degradation, conservation and rearrangement in the carbonisation of polyflavonoid tannin/furanic rigid foams—a MALDI-TOF investigation,” *Polymer Degradation and Stability*, vol. 93, no. 5, pp. 968–975, 2008.
- [15] G. Tondi, A. Pizzi, H. Pasch, A. Celzard, and K. Rode, “MALDI-ToF investigation of furanic polymer foams before and after carbonization: aromatic rearrangement and surviving furanic structures,” *European Polymer Journal*, vol. 44, no. 9, pp. 2938–2943, 2008.
- [16] A. Pizzi, G. Tondi, H. Pasch, and A. Celzard, “Matrix-assisted laser desorption/ionization time-of-flight structure determination of complex thermoset networks: polyflavonoid tannin-furanic rigid foams,” *Journal of Applied Polymer Science*, vol. 110, no. 3, pp. 1451–1456, 2008.
- [17] A. Reyer, G. Tondi, M. Demker, A. Petutschnigg, and M. Musso, *Journal of Raman Spectroscopy*, submitted.

- [18] A. Pizzi, "Tannin-based wood adhesives," in *Advanced Wood Adhesives Technology*, chapter 5, pp. 149–217, Marcel Dekker, New York, NY, USA, 1994.
- [19] A. E. Hagerman and L. G. Butler, "Tannins and lignin," in *Herbivores, Their Interactions with Secondary Plant Metabolites*, chapter 10, pp. 355–383, Academic Press, San Diego, Calif, USA, 1991.
- [20] M. Choura, N. M. Belgacem, and A. Gandini, "Acid-catalyzed polycondensation of furfuryl alcohol: mechanisms of chromophore formation and cross-linking," *Macromolecules*, vol. 29, no. 11, pp. 3839–3850, 1996.
- [21] M. Choura, N. M. Belgacem, and A. Gandini, "The acid-catalyzed polycondensation of furfuryl alcohol: old puzzles unravelled," *Macromolecular Symposia*, vol. 122, no. 1, pp. 263–268, 1997.
- [22] C. L. Burket, R. Rajagopalan, A. P. Marencic, K. Dronvajjala, and H. C. Foley, "Genesis of porosity in polyfurfuryl alcohol derived nanoporous carbon," *Carbon*, vol. 44, no. 14, pp. 2957–2963, 2006.
- [23] G. Tondi and A. Petutschnigg, "Middle infrared (ATR FT-MIR) characterization of industrial tannin extracts," *Industrial Crops and Products*, 2015.
- [24] R. T. Conley and I. Metil, "An investigation of the structure of furfuryl alcohol polycondensates with infrared spectroscopy," *Journal of Applied Polymer Science*, vol. 7, no. 1, pp. 37–52, 1963.
- [25] O. Unsalan, Y. Erdogdu, and M. T. Gulluoglu, "FT-Raman and FT-IR spectral and quantum chemical studies on some flavonoid derivatives: baicalein and Naringenin," *Journal of Raman Spectroscopy*, vol. 40, no. 5, pp. 562–570, 2009.
- [26] L. Ping, A. Pizzi, Z. D. Guo, and N. Brosse, "Condensed tannins from grape pomace: characterization by FTIR and MALDI TOF and production of environment friendly wood adhesive," *Industrial Crops and Products*, vol. 40, no. 1, pp. 13–20, 2012.
- [27] C. Song, T. Wang, X. Wang, J. Qiu, and Y. Cao, "Preparation and gas separation properties of poly(furfuryl alcohol)-based C/CMS composite membranes," *Separation and Purification Technology*, vol. 58, no. 3, pp. 412–418, 2008.
- [28] E.-M. A. Ajuong and C. Birkinshaw, "The effects of acetylation on the extractives of Sitka Spruce (*Picea sitchensis*) and Larch (*Larix leptoleptis*) wood," *Holz als Roh-und Werkstoff*, vol. 62, no. 3, pp. 189–196, 2004.
- [29] C. W. Oo, M. J. Kassim, and A. Pizzi, "Characterization and performance of *Rhizophora apiculata* mangrove polyflavonoid tannins in the adsorption of copper (II) and lead (II)," *Industrial Crops and Products*, vol. 30, no. 1, pp. 152–161, 2009.

